Ultrafast response micropipette-based submicrometer thermocouple

G. Fish, O. Bouevitch, S. Kokotov, K. Lieberman, D. Palanker, I. Turovets, and Aaron Lewis[a)]

Division of Applied Physics, The Hebrew University of Jerusalem, Jerusalem 91904, Israel

(Received 27 June 1994; accepted for publication 30 November 1994)

Submicrometer-size thermocouples at the tip of gold-coated glass micropipettes containing a platinum core were produced and tested. The response time of such thermocouples measured with different techniques appeared to be not bigger than a few microseconds. The calculations indicate that the spatial selectivity of this new class of thermocouple devices can be less than 2 μm along the pipette and less than 50 nm across the pipette. The suitability of this thermocouple for light intensity measurements with micrometer spatial resolution is demonstrated by measuring the focused beam of an argon-ion laser. In addition, such thermocouples are intrinsically suitable for applications in scanned probe microscopies. All these unique advantages make the pipette thermocouples a new and promising sensor in a variety of applications. © *1995 American Institute of Physics.*

I. INTRODUCTION

The measurements of spatially localized rapid temperature changes are required in studies of many physical and biological processes and objects. These can include such diverse subjects as turbulent flows, associated with processes of explosion and combustion, microtemperature measurements in biology at the cellular and subcellular level, microtemperature measurements in evolving chemical reactions and microthermal measurements in mesoscopic and other physical systems.

In recent publications, fast microthermocouples have been described with response times of milliseconds and spatial resolutions of from hundreds[1] to tens[2] of micrometers. Such microthermocouples may also be used as point radiation microdetectors in a range of wavelengths from the UV to the IR. For example, Srinivas *et al.*[3] produced and tested 20-μm fast infrared detectors made of a free-standing thermocouple. In the present paper, we advance these efforts in microtemperature measurements with a thermocouple with submicrometer contact size and a response time of a few microseconds. We demonstrate that a micropipette containing a platinum core can be coated with gold to make a gold–platinum point thermocouple at the tip of the micropipette. This unique submicrometer thermocouple structure was then characterized in terms of both its response time and its ability to image thermal gradients.

II. THEORETICAL CONSIDERATIONS

We first present a comparative analysis of the spatial resolution and the response time of known wire[1,2] and the micropipette-based thermocouples presented in this paper.

A. Wire and disk thermocouples

The equation that defines the heat exchange between an ordinary wire thermocouple and its surroundings can be written in the following form:

$$c\rho(\pi D^2/4)dT/dt = -\alpha\pi DT, \tag{1}$$

where c is the specific heat of the metal, ρ the density of the metal, T the difference between the medium and wire temperature, t the time, D the wire diameter, and α the heat transfer coefficient.

For liquids in the absence of flow and thin wires, it was found that the heat transfer coefficient depends on the wire diameter D as follows:[4]

$$\alpha \approx 0.24\lambda_m/D, \tag{2}$$

where λ_m is thermal conductivity of the liquid. In this case, the solution of Eq. (1) can be written as

$$T = T_0 \exp(-t/\Theta), \tag{3}$$

where $\Theta = D^2 c\rho/\lambda_m$ is the response time of a wire thermocouple. For a copper wire of diameter $D = 20$ μm in water [$\lambda_m = 0.6$ W/(m °C)] the response time Θ is 2 ms.

From the viewpoint of spatial resolution, a serious disadvantage of wire thermocouples is that temperature is sensed not only by the contact itself but also by wires near the contact. The area that in fact senses temperature can be calculated on the basis of the requirement that the longitudinal heat flow along the wire is much smaller than the heat flow from the medium to the wire surface:

$$\pi D^2/4(\lambda/L) \ll \pi DL\alpha, \tag{4}$$

where λ is the thermal conductivity of the wire material and L is the length of a sensing zone. The sign "$\ll$" that is found in Eq. (4) and in the evaluation of the parameters below assumes a difference of one order of magnitude. Thus the actual size of the temperature sensing area of a copper wire thermocouple in water is about 80× larger than the contact size. Therefore for a 20 μm thermocouple the area is as large as 1.6 mm.

To decrease the temperature sensing area and the response time, the general approach that is used is to increase the heat flow from a surface of a contact by flattening the contact. Beckman *et al.*[2] flattened the contact of two 20 μm wires into a disk with a diameter of 80 μm and a thickness of 2.5 μm. As a result, the sensing area of the thermocouple decreased to approximately the disk diameter (80 μm) and

a)To whom reprint requests should be addressed.
E-mail: LEWISU@VMS.HUJI.AC.IL

 0034-6748/95/66(5)/3300/7/$6.00

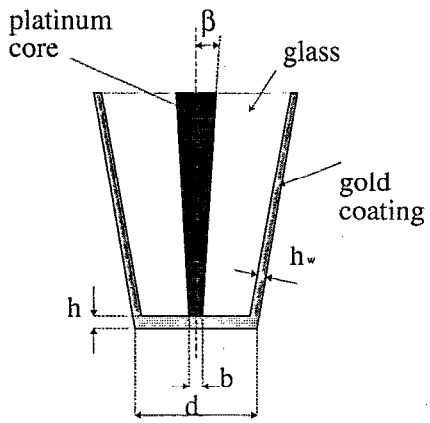

FIG. 1. Schematic presentation of the sensing area of the pipette thermocouple.

the response time decreased to 3 ms. These are the state-of-the-art parameters for thermocouples produced using wire-based technologies.

B. Pipette thermocouple

The analysis of heat distribution in our point thermocouple based on the micropipette technology that we introduce in this paper allows one to determine restrictions imposed on the geometry of such a thermocouple. These restrictions come from the requirement for the contact temperature to be close to the temperature of the surrounding medium. For this requirement to be achieved, undesirable heat flows through the gold coating on the walls of the pipette and through the platinum core should be minimized. This can be expressed in the following conditions restricting the geometry of the micropipette thermocouple shown in Fig. 1.

1. Condition 1

The heat flow through the platinum core should be smaller than the heat flow from the medium to the tip of the pipette. This condition, interpreted in terms of the solution of the heat transfer equation, leads to the following restriction imposed on the cone angle β:

$$\beta \ll \lambda_m d/(\lambda_{Pt} b), \tag{5}$$

where $\lambda_{Pt}=73$ W/(m °C) is the thermal conductivity of platinum, b the diameter of the platinum electrode at the contact, and d the pipette tip diameter. For this condition to be fulfilled, for $b/d=0.1$ in water, the cone angle β should be much less than 0.082 rad (4.8°).

2. Condition 2

The thermal conductivity of the gold coating at the tip should ensure the effective sensing temperature by the whole surface of the tip. Based on the solution of the heat transfer equation for a disk-shaped metal layer with heat outflow from its center, this condition takes the form

$$\lambda_{Pt}(b/2)\beta \ln(d/b) \ll 2h\lambda_{Au}, \tag{6}$$

where h is the thickness of the gold disk (see Fig. 1) and $\lambda_{Au}=315$ W/(m °C) is the thermal conductivity of gold. This yields $h/d \gg 2\times10^{-4}$ for $b/d=0.1$ and $\beta=1°$.

In the case where conditions 1 and 2 are satisfied, the spatial resolution of the pipette thermocouple can be evaluated as

$$\pi d h_w \lambda^*_{Au}/L \ll 0.24\pi L \lambda_m, \tag{7}$$

where λ^*_{Au} is the longitudinal thermal conductivity of a gold coating of thickness h_w. The thermal conductivity λ of a metal is proportional to its electrical conductivity Λ, and Λ of thin metal films is always smaller than Λ of bulk metal.[5] For a gold film with a thickness of less than 0.05 μm, Λ is one or two orders of magnitude smaller than the bulk Λ depending on the deposition rate.[5] By taking this into consideration, for a 300 Å thick gold coating of a 0.5 μm pipette in water we obtain $L \approx 2$ μm. The last value is much smaller than that of the sensing area of the disk[2] and wire[1] thermocouples.

The response time of the pipette thermocouple with the above mentioned dimensions according to formula (3) is as small as $\Theta=0.7$ μs for the measurements in water. Thus the pipette thermocouple allows us to improve both the response time and the spatial resolution.

III. THERMOCOUPLE FABRICATION

In order to obtain optimal parameters of a thermocouple, it is necessary, as has been shown in Sec. II, to reduce the size of the sensor d, the thickness of the gold coating h_w, and the cone angle of the platinum core β. At present, a number of methods are available for producing microelectrodes, such as electropolished platinum, carbon sealed in glass, and other methods.[6–9] However, all these methods are not easy to reproduce technologically, and the yield of satisfactory electrodes is low. Pendley and Abruna[10] described an elegant method of microelectrodes fabrication which involves pulling an annealed platinum wire placed inside a borosilicate pipette by a common pipette puller. However, the authors of Ref. 10 were not able to control the parameters of the cone.

We describe here a technique for the production of microelectrodes which allows one to control and vary its parameters. The reproducibility of this technique is about 90%. A platinum wire, 80 μm in diameter, was placed inside a borosilicate tube with outer and inner diameters equal to 1.2 and 0.3 mm, respectively. The pipette wire assembly was placed in a Sutter P-2000 laser pipette puller which allowed varying of five parameters: temperature of heating, the length of the segment heated, delay time between turning the heat on and the beginning of pulling, the velocity of the pull, and the strength of the pulling.

To find the optimal combination of these parameters, we treat our sample, consisting of a glass tube and a platinum wire inside it, as a composite material (CM). In this material the heated glass tube acts as the matrix which is more plastic than the platinum wire which acts as the frame. During the pulling procedure the surrounding glass acts to stabilize the metal and thus results in a more uniform thinning of the

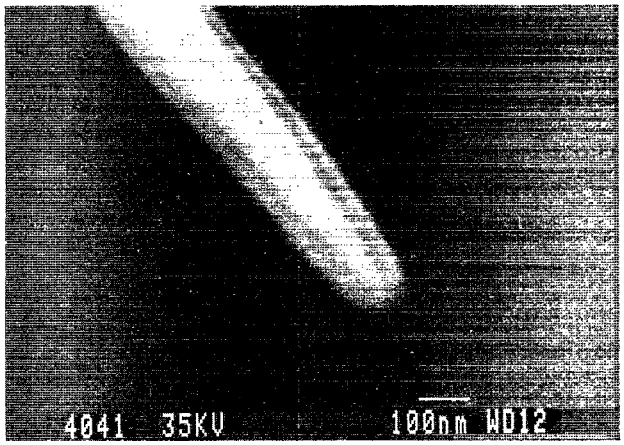

FIG. 2. Scanning electron micrograph of a platinum filled micropipette. Bar, 100 nm.

metal core. Therefore the metal core can be pulled down to a smaller dimension before the breaking occurs.

It is also known that for CMs of this type there is some critical volume fraction of the frame, V_{cr}, at which the plasticity of the CM becomes equal to that of the surrounding matrix, i.e., glass in this particular case. Note that the platinum wire diameter D_w was not varied, while the external diameter of the glass tube D_{gl} depended on parameters that were set for the pulling program. Since the ratio $A \equiv D_w/D_{gl}$ defines the volume fraction V of the frame, we can ensure $V \approx V_{cr}$ by simply varying D_{gl}. We therefore performed the pulling operation in the following two steps.

First, the glass tubes were pulled to an inner diameter that was equal to the platinum wire diameter. At this point the sample was heated for several seconds without further pulling to ensure a firm connection between the glass and the platinum.

Subsequently, the pulling was performed slowly, in four stages, and this resulted in the formation of two glass pipettes that were filled with platinum to the end. The shape of the cone and the outer diameter was determined by the pulling program parameters at both steps. At $0.2 < A < 0.4$, it was possible to pull the glass tube and the platinum core to dimensionalities as small as 50 nm. Figure 2 shows a scanning electron micrograph of such a microelectrode. The Pt electrode is clearly seen when the glass at the tip is etched back. In Fig. 3, microelectrodes of different shapes, obtained with the use of the above-mentioned technology, are shown.

The second thermoelectrode was made as a vacuum-evaporated thin gold film. The pipette tip was facing the gold source. Using this geometry, we succeeded in producing edgelike coatings with a maximal thickness of the gold layer near the tip to fulfill condition 2 in the theoretical discussion above. Varying the rate and time of deposition, we obtained coatings with the required thickness and electrical conductance.[5] This enabled us to improve the spatial resolution of our thermocouples (see previous section).

The sensitivity of the microthermocouples produced was about 7 μV/ °C, which is slightly less than that of a bulk gold–platinum thermocouple.[11]

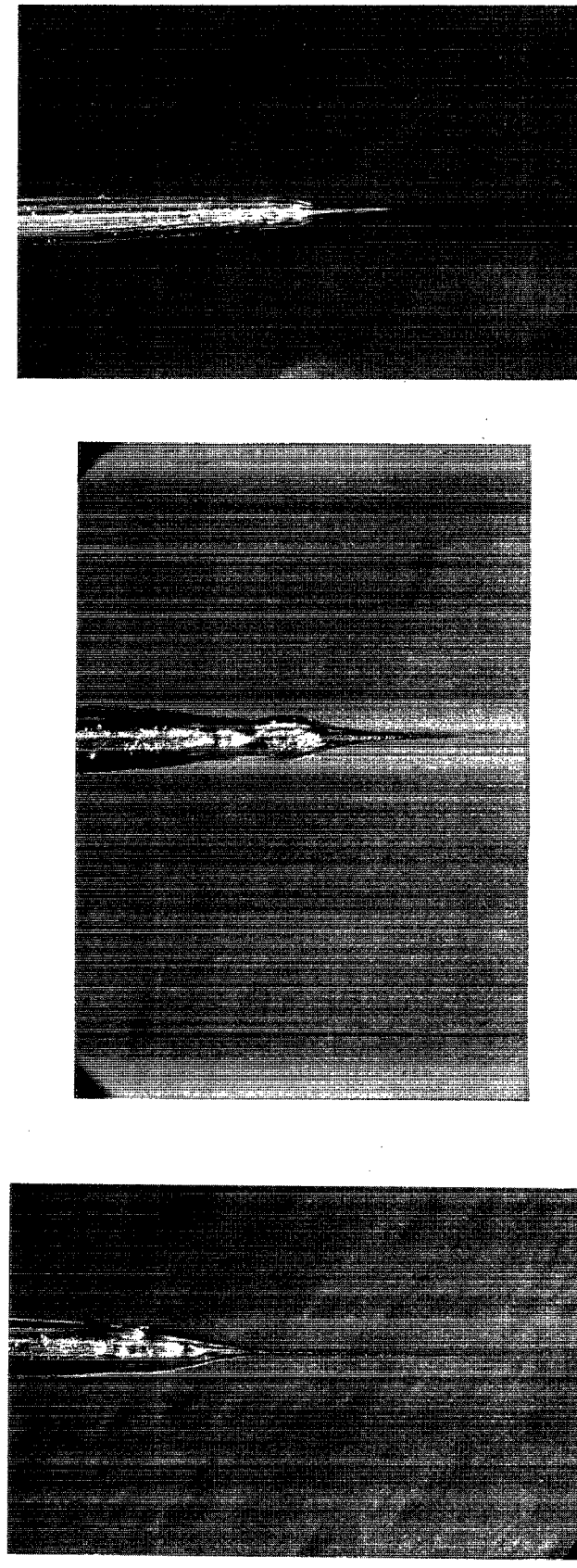

FIG. 3. Light micrographs of pipette thermocouples with different shapes. The magnification is ×50.

IV. KINETIC MEASUREMENTS

A. Direct laser heating

The kinetic experiments were aimed at determining the response time of the pipette thermocouples. Initially we chose a technique which was based on direct laser heating of the thermocouple. The measurements were performed as follows. The thermocouple was immersed in a medium, of water or air with no obvious convection, and illuminated with submicrosecond pulses of a near-infrared Nd:YAG laser light source. As a result of illumination, a temperature difference was created between the thermocontact and the medium since only the thermocontact region of the thermocouple absorbed heat while the media were practically transparent at the wavelength of this laser, 1.064 μm. The kinetics of the subsequent cooling of the thermocontact was determined by measuring the thermocurrent with submicrosecond time resolution.

The Q-switched Nd:YAG laser used as the pulsed heat source yielded 300 ns, 1 mJ pulses at a repetition rate of 100 Hz. The emission of the laser was focused by a lens onto the pipette tip so that the pulse energy density of the infrared light was 0.5–2 J/cm^2. A part of the laser emission was directed to a pin photodiode. The thermocouple output was amplified by a factor of 25 by a pair of Stanford Research model 240 preamplifiers which have an input resistance 50 Ω and a bandwidth 0 Hz–100 MHz. Both signals, from the photodiode and the amplified thermocouple output, were processed by an identical pair of Stanford Research model 250 gated integrators and boxcar averagers. During the experiment, the delay time between the laser pulse and the identical pair of gate pulses from the gated averagers was continuously scanned in the region of -1 to $+6$ μs, and the outputs of the averagers were digitized and stored in a microcomputer. Two curves were recorded simultaneously. One of them, obtained with the use of the fast photodiode, served as the instrumental response function (IRF) of the system, and the second represented the response of the thermocouple to laser heating. To estimate the response time of the thermocouple which was measured as the rate of cooling of the thermocouple after the laser pulse, one has to deconvolve the second curve using the first one as a system IRF.

The results of the kinetic measurements performed with three different pipette thermocouples, are shown in Fig. 3, are presented in Fig. 4. The thermocouples 1, 2, and 3 had tip diameters of about 3, 1, and 0.5 μm and the cone angle β was equal to 5°, 2°, and 1°, respectively. In the discussion below, we refer to thermocouples 1, 2, and 3 as "thick," "intermediate," and "thin," respectively. In each figure, three curves are shown. The first curve, shown as a dashed–dotted line, is the system IRF. The second and third curves, shown in dotted and solid lines, represent the thermocouple output as a result of laser heating in air and in water, respectively. (A spike seen in thermocouple outputs just before arrival of the laser pulse is an artifact which is probably caused by interference from the Q-switcher of the laser.) From Fig. 4, it is seen that (1) the response times of all thermocouples are of the order of a few microseconds, (2) these response times are smaller for thinner pipette thermocouples, and (3)

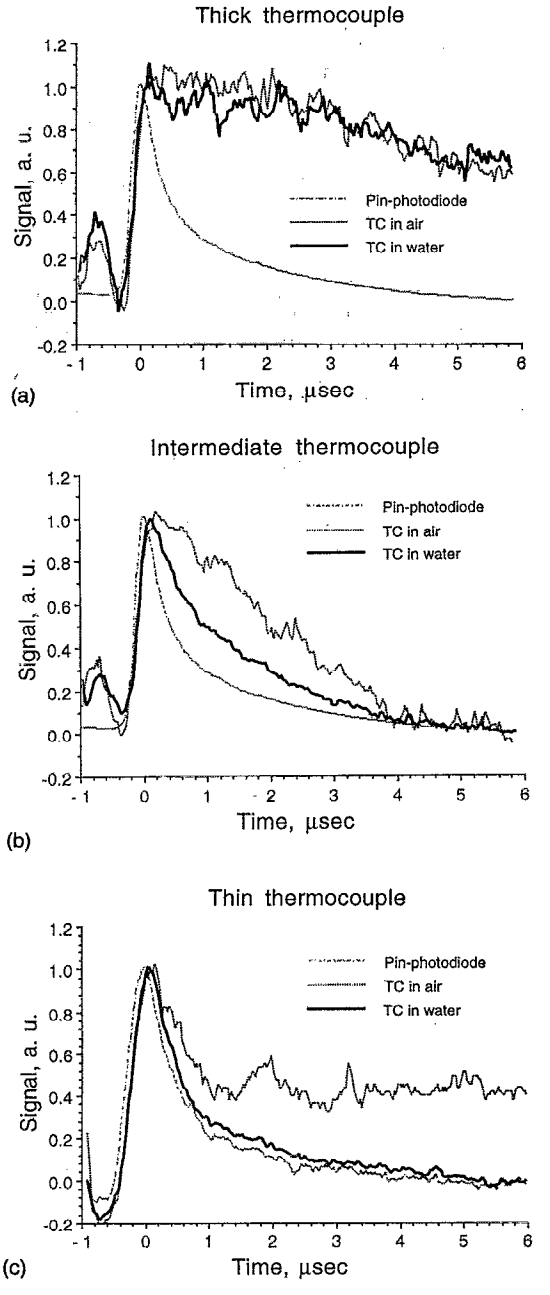

FIG. 4. Response of (a) thick, (b) intermediate, and (c) thin thermocouples to direct laser heating. Dashed–dotted line, the signal from a pin photodiode; dotted and solid lines, the signal from a thermocouple immersed in air and water, respectively. The photodiode output represents the heating laser pulse.

the thinner the pipette and the smaller the cone angle, the larger the influence of the environment (water or air) on the thermocouple's output kinetics. For instance, the thick thermocouple, shown in Fig. 4(a), has similar response times in water and in air, about 15 μs, whereas the thinner thermocouples 2 and 3 [Fig. 4(b) and 4(c), respectively] are faster in water than in air. The response time of the intermediate thermocouple is close to 1.0 and 2.2 μs and the response time of thin thermocouple is <0.4 μs in water. Two components are seen in the exponential decay in Fig. 4(c) for the case of the cooling of the thin thermocouple in air, the first component having a response time of about 1 μs. The experiments per-

formed on longer time scales have shown that the decay time of the second component is not smaller than 10–15 μs. All values of response times mentioned here have been corrected for the finite IRF of the system. The data presented demonstrate that the temporal characteristics of the pipette thermocouples can be readily controlled by choosing the appropriate outer diameter of the tip.

The observed difference of cooling kinetics in air and in water for different thermocouples probably results from the following. For a thick thermocouple, heat produced by laser illumination of the thermocouple dissipates mainly via the platinum core because of its large cone angle, so that the relaxation time does not depend on the environment. For intermediate and thin thermocouples, heat dissipates mainly through the gold surface, and this explains why the response time of these thermocouples depends on the environment. For instance, the dotted curve seen in Fig. 4(c) has a long "tail," while the solid curve does not, which indicates that the heat exchange between the thin thermocouple and the air is not complete after 6 μs, in contrast to the measurements in water, where the heat exchange seems to follow the temporal nature of the heating pulse. Heat dissipation via the platinum core is probably hindered for intermediate and thin thermocouples by a small cone angle of the intermediate and thin pipettes, as indicated in the theoretical consideration above. For the thin thermocouple, which is as thin as 0.5 μm, an apparent response time of less than 400 ns is obtained for the case when the thermocouple is immersed in water.

Nonetheless, we do not exclude the possibility that a 300 ns pulse is not long enough to create uniform heating of the thermocouple. In this case, the temperature-sensing area of the thermocouple would not be heated uniformly. The heat flow within the metallic layers in the region of the thermocontact which would follow such nonuniform heating could probably distort the true thermocouple cooling kinetics. Experimental observations indicate, however, that this effect seems unlikely to take place, since the initial submicrosecond stages of the decay of the signal from a thermocouple immersed in air and in water clearly differ from one another [compare dotted and solid curves in Fig. 4(b) and 4(c)] and this means that the cooling of the thin thermocouple during the first microseconds after the laser flash does come from the heat exchange with the surrounding water layers. In spite of the fact that we have achieved a qualitative understanding of the kinetics of cooling of these thermocouples, the biexponential relaxation of the thin thermocouple output for the case of cooling in air is not fully understood.

B. Study of a laser-induced cavitation bubbles

To demonstrate the possibility of real time measurements of fast thermal processes, we performed the following experiment. The aqueous solution of NaCl at a concentration of 100 g/ℓ was heated with 20 ns pulses of an excimer laser at a wavelength of 193 nm delivered via a specially prepared optical fiber. The energy fluence at the exit of the fiber $F=0.35$ (J/cm^2)/pulse was high enough to evaporate the water layers in the vicinity of the fiber exit as a result of absorption of the ultraviolet light energy by chloride ions present in solution. This produced vapor bubbles in the liquid. These bubbles grew to 600 μm in diameter on the time scale of 20–30 μs and then collapsed.[12] The signal from the thermocouple held at a set distance from the fiber exit was processed as in previous experiments, and in addition, a digital sampling oscilloscope, Tektronix TDS520, was used to collect the data. A petri dish with a salt solution was mounted on an inverted optical microscope. A fiber and a microthermocouple, held by micromanipulators, were immersed into the solution. The microscope was equipped with a computer-controlled CCD camera, and a Candela flash-lamp pumped dye laser having a pulse duration of 350 ns was used for visualization of the bubble. This laser was synchronized with the bubble-producing excimer laser. This experimental arrangement, which we describe in detail in Ref. 12, allowed us to obtain real time images of different stages of bubble formation with 0.5 μs time resolution. The four photographs presented in Fig. 5 are taken at 0, 3, 5, and 23 μs after the excimer laser pulse, as indicated in the lower left corner of each photograph. By comparing the time course of the thermoelectric signal, generated by the thermocouple, with such fast photographs, we were able to attribute changes in the thermoelectric signal to changes in the character (liquid or gas) of the environment of the thermocouple as discussed below.

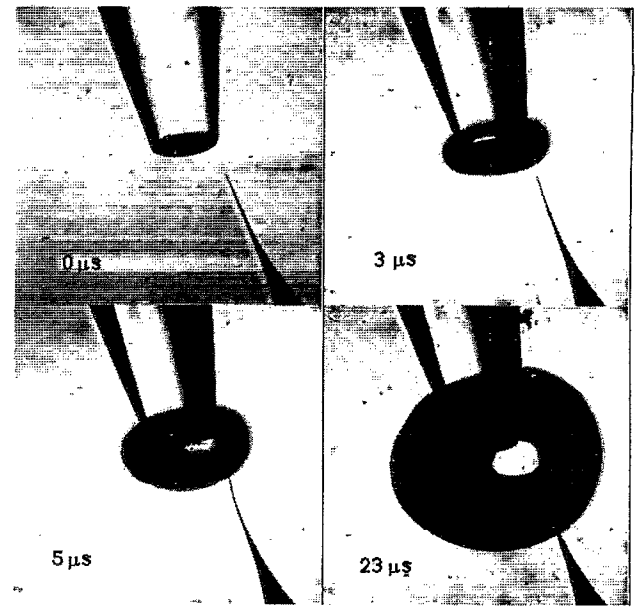

FIG. 5. Photomicrographs illustrating the process of bubble formation. Numbers in the left bottom corner of every picture represent the time delay between the ultraviolet laser pulse that forms the bubble and the illuminating flash used to photograph the bubble.

The bubble was already seen 3 μs after the 193 nm excimer laser pulse (Fig. 5). It reached the thermocouple that was at a distance of 300 μm from the fiber tip in less than 5 μs, so that in 23 μs the thermocontact was already in the gas phase, i.e., within the bubble. In approximately 50 μs, the bubble contracted completely, and the thermocouple tip was again in liquid phase.

Let us turn now to the thermoelectric signals detected, which are shown as a function of time in the graphs in Fig.

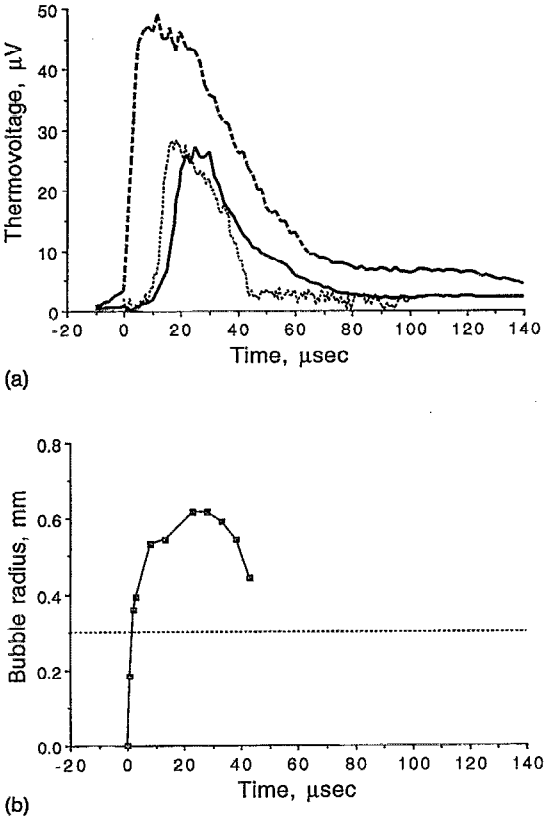

FIG. 6. (a) Response of thick and thin thermocouples to heating by the laser-induced bubble. Three graphs are shown in this picture. The graph shown in thick dashed line represents, as a function of time, the output signal of a thick thermocouple placed at a distance of 30 μm from the tip of the UV emitting fiber. The two remaining graphs, shown, respectively, as thick solid and thin dashed lines, are the outputs of the thick and thin thermocouples at a distance of 300 μm, respectively. (b) In this graph, the radius of the bubble, measured by fast photography, is plotted as a function of time. The dotted horizontal line in this graph marks the distance of 300 μm from the fiber tip. Comparison of the two graphs, (a) and (b), allowed us to establish a connection between the dynamics of bubble formation and the signals that were obtained from the thermocouples.

6(a). The 20 ns excimer laser pulse arrives at zero time. The two curves drawn in thick solid and thin dotted lines represent the time course of the thermoelectric signal from thick and thin thermocouples, respectively, when the distance between the center of the fiber exit and the tip of the pipette thermocouple was equal to 300 μm. The highest curve, shown in thick dashed line, is the signal from thick thermocouple for the case when the thermocontact was brought closer to the UV fiber tip, to a distance of about 30 μm. The thin thermocouple, brought to the same distance, was broken by a bubble.[13] The graph in Fig. 6(b) shows, as a function of time, the radius of the bubble measured as distance from center of fiber tip to the boundary of the bubble. The dashed horizontal straight line in the bottom graph marks the distance from the fiber tip to the microthermocouple equal to 300 μm.

By correlating the signals in Fig. 6(a) and 6(b), we can assume that the thermocontact is mostly heated by condensation of vapor inside the bubble onto the pipette tip. Indeed, as the bubble grows, the vapor temperature and density decrease, explains both the decrease of the value and the increase of the rise time of the thermoelectric signal with the distance from the heat source. At some moment after thermocontact appears in the vapor phase, the heating seems to stop. At approximately 30 μs the signal starts to decay with a characteristic time of about 10 and 18 μm for thin and thick thermocouples, respectively. These values are in a good agreement with the results obtained when heating of thermocouples was performed with the emission of a Nd–YAG laser in air.

It should be mentioned that it is problematic to treat the signals presented in Fig. 6(a) as a real temperature changes inside the bubble. In the case of a vapor environment, condition 1 and Eq. (5) in the theoretical section are not satisfied because of small thermal conductivity of the vapor (λ_{vapor} is approximately 20× smaller than λ_{water}). The experimentally observed rise times of the signals are much smaller than expected from Eq. (3) for λ_{vapor}. One of the possible explanations of the observed signals is that the heat is transferred to the thermocouple by a condensation of the vapor. Indeed, the heat transfer coefficient of a condensing vapor is much higher than that of water,[14] which explains the fast rise time of the signals. Time delays of about 5–10 μs between the moment when the bubble reaches the thermocouple tip and the moment of the rise of the thermocouple signal, clearly seen by comparison of Fig. 6(a) with 6(b), can be understood because the effective condensation starts only when the vapor is overcooled, and this is realized at some stage of the expansion of the initially overheated vapor bubble.

Thus, in these experiments we show that our thermocouple enables one to thermally detect and monitor on a microsecond time scale thermal processes such as water vapor bubble formation.

V. IMAGING WITH THE MICROPIPETTE THERMAL PROBE

One of the possible applications of microthermocouples is in microthermal imaging. To test the imaging capabilities of our thermal probe we placed the micropipette into a near-field scanning optical microscope[15] that was specifically designed for working with micropipette probes. Our initial images were obtained by scanning the tip through a laser beam focused to an approximately 2 μm spot by a Zeiss microscope with a 50× magnification, 0.5 NA, long working distance, and infinity corrected objective. The infinity corrected objective allowed us to focus the beam onto the tip by simply viewing the tip through the microscope. The voltage on the probe was recorded with a Keithley 182 microvoltmeter via a GPIB interface. The imaging software was modified to acquire voltage data in synchronization with the probe scanning.

A thermal image of the laser spot produced with a platinum/gold micropipette with a tip of approximately 2 μm is shown in Fig. 7. The full scan range is 9 μm. The few milliwatts of laser light produced a maximum temperature of 150 °C at the center of the spot. The laser beam was slightly off the optical axis of the objective and this produced a weak residual heating of the probe on one side as it passed through the spot. This smear can be seen in the image. The acquisition time for this image was limited not by the thermal re-

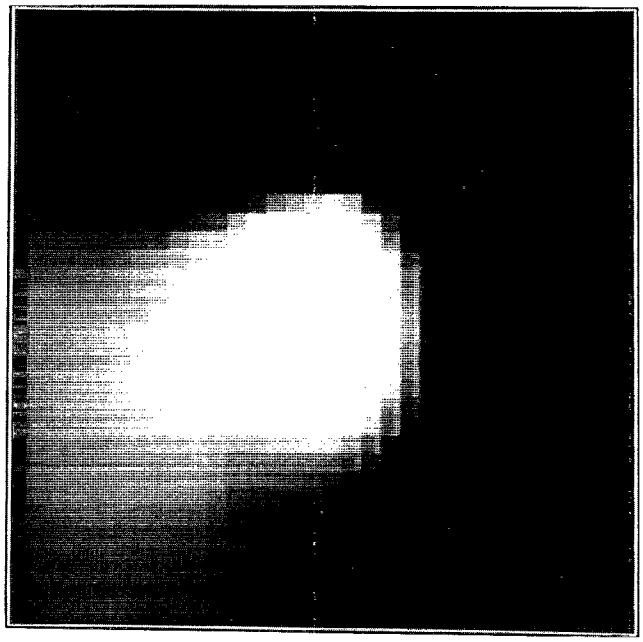

FIG. 7. Thermal image of the focal spot of an Ar^+ laser beam. The full scan range is 9 μm.

sponse of the probe, which can be on the order of microseconds as described above, but by the settling time of the microvoltmeter used to record the temperature, which was on the order of 100 ms.

In order to make use of the micropipette thermal sensors for general imaging of surfaces, it is advantageous to incorporate a feedback mechanism as is commonly used in scanned probe microscopes. In this regard it is important to note that micropipettes have been used as probes in many forms of scanned probe microscopy including tunneling[15] and force microscopy.[16] Recent results with cantilevered micropipettes[17] have demonstrated that such probes are uniquely suited for all forms of scanned probe microscopy. We have succeeded in producing such cantilevered structures with metal filled thermal micropipette sensors and work is currently under way to incorporate these probes into scanned force microscopes. The simultaneous topographic and thermal imaging that this will allow should produce a very powerful tool. Many applications are possible including imaging microelectronic circuits while they are operating in order to detect localized heating as a result of linewidth variations or defects in fabrication.

[1] L. J. Forney, E. L. Meeks, J. Ma, and G. C. Fralick, Rev. Sci. Instrum. **64**, 1280 (1993).
[2] P. Beckman, R. P. Roy, K. Whitfield, and A. Hasan, Rev. Sci. Instrum. **64**, 2947 (1993).
[3] T. A. S. Srinivas, P. J. Timans, R. J. Butcher, and H. Ahmed, Rev. Sci. Instrum. **64**, 3602 (1993).
[4] R. A. Antonia, L. W. B. Browne, and A. J. Chambers, Rev. Sci. Instrum. **52**, 1382 (1981).
[5] M. Adamov, B. Perovic, and T. Nenadovic, Thin Solid Films **24**, 89 (1974).
[6] R. M. Dowben and J. E. Rose, Science **118**, 22 (1953).
[7] C. M. Ballintizn, Experimentia **17**, 523 (1961).
[8] A. Meulemans, B. Poulain, G. Baux, L. Tauc, and D. Henzel, Anal. Chem. **58**, 2088 (1986).
[9] W. J. Whalen, J. Riley, and P. Nair, J. Appl. Physiol. **23**, 798 (1967).
[10] B. D. Pendley and H. D. Abruña, Anal. Chem. **62**, 782 (1990).
[11] M. Gotoh, K. D. Hill, and E. G. Murdock, Rev. Sci. Instrum. **62**, 2778 (1991).
[12] I. Turovets, D. Palanker, and A. Lewis, Photochem. Photobiol. **60**, 412 (1994).
[13] It does not seem surprising that a glass micropipette can be broken by a bubble. Cavitation bubbles were known a long time ago [J. W. Rayleigh, Lord, Philos. Mag. **34**, 94–98 (1917)] to cause a significant damage even to such objects as screw propellers of ships! At present, the laser-induced cavitation bubbles are used in laser surgery [see A. Vogel, P. Schveiger, A. Frieser, M. N. Asiyo, and R. Birngruber, IEEE Quantum Electron. **26**, 2240 (1990)] for mechanical cutting of tissues.
[14] H. Kuchling, *Physik Handbook* (Veb Fachbuchverlag, Leipzig, 1980).
[15] K. Lieberman and A. Lewis, Appl. Phys. Lett. **62**, 1335 (1993).
[16] S. Shalom, K. Lieberman, A. Lewis, and S. R. Cohen, Rev. Sci. Instrum. **63**, 4061 (1992).
[17] K. Lieberman, A. Lewis, G. Fish, T. Jovin, A. Schaper, and S. R. Cohen, Appl. Phys. Lett. **65**, 648 (1994).